ARTICLES
PUBLISHED ONLINE: 28 APRIL 2013 | DOI: 10.1038/NGEO1789
nature geoscience

Permanent deformation caused by subduction earthquakes in northern Chile

A. Baker[1], R. W. Allmendinger[1]*, L. A. Owen[2] and J. A. Rech[3]

Earthquakes are accompanied by coseismic and post-seismic rebound: blocks of crust on either side of the fault spring back to their initial, undeformed configuration. This rebound is well documented by space geodetic data, such as the Global Positioning System. Thus, all earthquake-induced deformation of the crust is considered non-permanent and is modelled as an elastic or visco-elastic process. Here, however, we show that earthquakes larger than magnitude 7 in northern Chile caused the crust to deform permanently. We identify millimetre- to metre-scale tension cracks in the crust of the Atacama Desert and use cosmogenic nuclides to date the timing of crack formation. The cracks were formed by between 2,000 and 9,000 individual plate-boundary earthquakes that occurred in the past 0.8–1 million years. We show that up to 10% of the horizontal deformation generated during the earthquakes, recorded by Global Positioning System data and previously assumed to be recoverable, is permanent. Our data set provides a record of permanent strain in the shallow crust of the South American Plate. Although deformation of the deep crust may be predominantly elastic, we conclude that modelling of the earthquake cycle should also include a significant plastic component.

The elastic rebound concept for earthquakes was first introduced by Harry Fielding Reid[1] in his study of the 1906 San Francisco earthquake and has dominated our understanding of the seismic cycle ever since, although we now know that some of the rebound occurs over months to decades following a major earthquake and thus can have a significant viscoelastic component[2,3]. The earthquake cycle along subduction zones is likewise commonly interpreted in terms of elastic rebound although, because of the orientation of the fault plane, coseismic vertical displacements are opposite to interseismic displacements as shown by numerous Global Positioning System (GPS) studies. In either case, the deformation of the rocks on either side of the fault that produced the earthquake is considered to be immediately or eventually recoverable and thus non-permanent. Sea level is a sensitive indicator of permanent vertical uplift[4]; however, the horizontal strains associated with co- and post-seismic deformation from a single event are small (of the order of 10^{-5}–10^{-6} at distances of tens of kilometres from the earthquake fault) and any permanent deformation would normally be exceedingly difficult to detect in the geological record. The hyperarid Atacama Desert of northern Chile (Fig. 1) may be the only place in the world where such permanent deformation can be preserved and identified. The subtle and delicate features produced during major plate-boundary earthquakes are preserved in geomorphic surfaces that routinely yield Pliocene and Miocene terrestrial cosmogenic nuclide (TCN) ages[5–8].

The Nazca–South America subducting plate boundary is responsible for some of the largest earthquakes over the past 100 years, including the 1960 Valdivia (M_w 9.5) and the 2010 Maule (M_w 8.8) earthquake. In northernmost Chile, a M_w 8.1 earthquake affected the Antofagasta region in 1995, and in southern Peru, the Arequipa region was struck by a M_w 8.5 event in 2001 (refs 9–11). The region between these two areas, known as the Iquique Gap (Fig. 1), has not had a major earthquake since the great earthquakes of 1868 and 1877 (refs 12–14). The southern part of the Iquique Gap did experience the M_w 7.7 Tocopilla earthquake in 2007, which released less than 5% of the moment accumulated since 1877 (refs 15,16).

Geodetically measured rates of convergence between Nazca and South America are about 63 mm yr^{-1} along an azimuth of 079° (refs 17,18). Thus, on average about 6 m of convergence occurs every century and, depending on the degree to which the subduction zone is locked along the seismic coupling interface, as much as 8 m of convergence have accrued since the last major earthquake in the Iquique Gap. This amount of slip is similar to that calculated previously[19] for an average Iquique earthquake (Fig. 1), based on the distribution and orientation of co/post-seismic cracks. These features are common in the Coastal Cordillera, which overlies the down-dip tip of the coupling zone.

Co/post-seismic cracks

The forearc of northern Chile and southern Peru preserves an extensive suite of cracks that are particularly well preserved in the saline soils that characterize the Atacama Desert[19–22]. These cracks have a variety of morphologies and origins; we report here on those that are known or inferred to be due to the seismic cycle based on: in mine excavations they have been observed cut at least 10 m into the Mesozoic basement rocks rather than being restricted solely to the saline soils; individual cracks have a relatively straight surface trace that can be tracked for hundreds of metres up to a few kilometres in the case of particularly large cracks; they are unrelated to local surface slopes and down-slope motion; the cracks exhibit systematic orientations over 500 km or more parallel to the Coastal Cordillera[19]; and the cracks have been observed to have formed during earthquakes[20,21,23,24] (see photographs in the Supplementary Information). We observed and measured cracks that probably formed during the 2007 Tocopilla earthquake in the course of our study.

[1]Department of Earth and Atmospheric Sciences, Cornell University, Ithaca 14853, New York, USA, [2]Department of Geology, University of Cincinnati, Cincinnati, Ohio 45221, USA, [3]Department of Geology and Environmental Earth Science, Miami University, Oxford, Ohio 45056, USA.
*e-mail: rwa1@cornell.edu

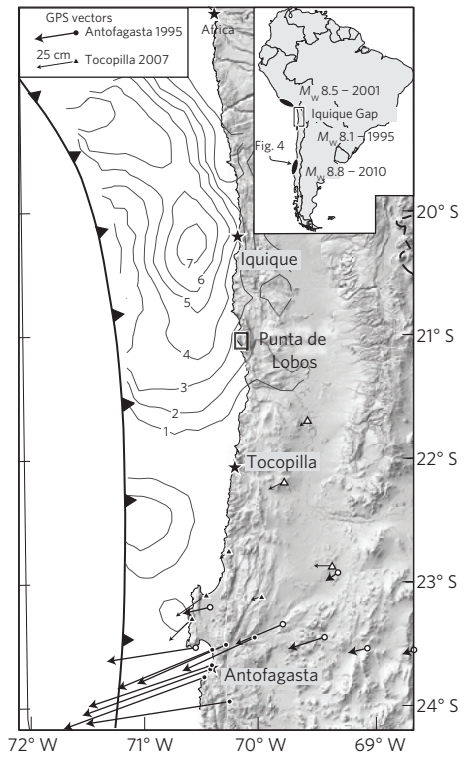

Figure 1 | Location of the study area, Punta de Lobos, in northern Chile. The barbed line is the Peru–Chile Trench. Contours show best fitting, long-term rupture segment for the Iquique Gap from ref. 19; numbers indicate slip magnitude in metres. Co/post-seismic GPS vectors for the 1995 Antofagasta earthquake (stations shown with circles) and the 2007 Tocopilla earthquake (triangles) shown at the same scale[15,36]. Filled station symbols indicate that the vector was used in the strain calculation in Fig. 5. Inset map shows the location, with the Iquique Gap bounded by the 2001 M_w 8.5 Arequipa earthquake to the north and the 1995 M_w 8.1 Antofagasta earthquake to the south.

The exact cause of earthquake-related cracking remains uncertain. The approximate north–south strike of most cracks[19] is consistent with static coseismic rebound of the upper plate. On the other hand, the common, although not exclusive association of the dense regions of cracking with forearc fault scarps and other topographic features indicates focusing during dynamic wave propagation[25]. In an ideal world, cracks formed by the latter mechanism would tend to close up resulting in little or no permanent strain. In the real world, however, there is abundant evidence, especially when seen in cross-section, that rock clasts fall into the cracks while open. Such clasts may act to prop open the cracks, creating much larger permanent surface strains than might otherwise be observed. We do not have sufficient temporal resolution to distinguish between cracks formed during the coseismic elastic rebound and those formed during the post-seismic recovery; from a geological perspective, the more important distinction is whether the deformation is permanent or recoverable (either immediately or over time).

Crack strain and strain rate

On a set of alluvial fan surfaces in the Coastal Cordillera at Punta de Lobos (Fig. 1), we measured ~7 km of scan lines over 5 surfaces (see Supplementary Information for details). Crack strain is calculated and reported here as a one-dimensional (1D) extension:

$$e = \frac{l_f - l_i}{l_i} = \frac{\Sigma W_h}{l_f - \Sigma W_h}$$

where l_f and l_i are the final and initial lengths, respectively, and ΣW_h is the sum of the crack widths along the transect as determined above. Crack strain clearly varies with alluvial fan surface age, with the oldest surfaces recording as much as 3.5% extension and the youngest surfaces registering less than 1% extension (Fig. 2).

Sufficient quartz clasts were available on three separate surfaces to determine their exposure ages from TCNs using ^{10}Be and ^{26}Al (see Supplementary Information for complete details). The oldest surface (S1) has an average age of 0.98 ± 0.18 Myr for all ^{10}Be and ^{26}Al ages; the intermediate surface (S2) has an average age of 0.35 ± 0.13 Myr; and the youngest surface (S5) an average age of 0.16 ± 0.08 Myr. ^{10}Be and ^{26}Al ages for pebbles and sediment in the active channels and quartz pebbles on the pediment and bedrock range from ~0.07 to 0.30 Myr suggesting that inheritance levels for cosmogenic nuclides of clasts and sediment on alluvial fan surfaces are of that order.

The dating of the surfaces, albeit with considerable uncertainty inherent in the technique, allows us to determine not just strain but strain rate (Fig. 3). Within the limits of error (discussed in the Supplementary Information), the strain rate seems to be relatively constant at about $1.2–1.5 \times 10^{-15}$ s^{-1} for 0.8–1 million years. If we assume that, on average, there is a major plate-boundary earthquake in the Iquique Gap every 150 ± 50 years[13], then the Punta de Lobos fan complex records between 2,000 and 9,000 individual events and the surface extension for each event, on average, is $7.1 \pm 2.3 \times 10^{-6}$. If we double the recurrence interval to 300 ± 50 years, the average per event strain would be $14.2 \pm 2.3 \times 10^{-6}$.

Comparison to GPS co/post-seismic strain

As the Iquique segment in which Punta de Lobos is located has not had a major earthquake since 1877, we must compare the per event strain calculated above to the GPS record of recent earthquakes in other parts of the margin. Furthermore, our crack strain measure is 1D and therefore we should compare it to horizontal strain along a GPS transect in the direction of maximum extension. Three recent earthquakes along the Nazca–South America plate boundary that were well captured by GPS networks include the 2010 M_w 8.8 Maule (Fig. 4), 1995 M_w 8.1 Antofagasta and 2007 M_w 7.7 Tocopilla events (Fig. 1). As expected, the maximum co/post-seismic extensions, measured in the 50 km immediately east of the coast, vary with magnitude of the earthquake: $4.8 \pm 0.65 \times 10^{-5}$ for Maule, $7.7 \pm 1.9 \times 10^{-6}$ for Antofagasta and $2.2 \pm 0.89 \times 10^{-6}$ for Tocopilla (see the Supplementary Information for calculation of strain for each event). These geodetically measured strains are very similar to the average per event strains calculated for the Punta de Lobos data based on 150 and 300 year recurrence intervals (Fig. 5).

Implications for coseismic deformation

If the crack strain we have documented were homogeneous over the entire Coastal Cordillera, it would suggest that a very high proportion of the rebound seen in GPS networks (12–27% for a Maule-sized event and nearly 100% for an Antofagasta-sized event) is actually due to permanent deformation and is not elastic or viscoelastic. However, there are two reasons why this is probably not the case: the crack strain in the Coastal Cordillera is probably not homogeneous; and we cannot rule out the effect of tectonic processes other than plate-boundary seismicity that might contribute to the strain measured at Punta de Lobos. We briefly examine both possibilities, below, ignoring Tocopilla as it is considerably smaller than an average 150 or 300 year event.

To determine the minimum amount that permanent crack strain at Punta de Lobos might contribute to the total coseismic rebound, it is necessary to compare changes in length rather than strain

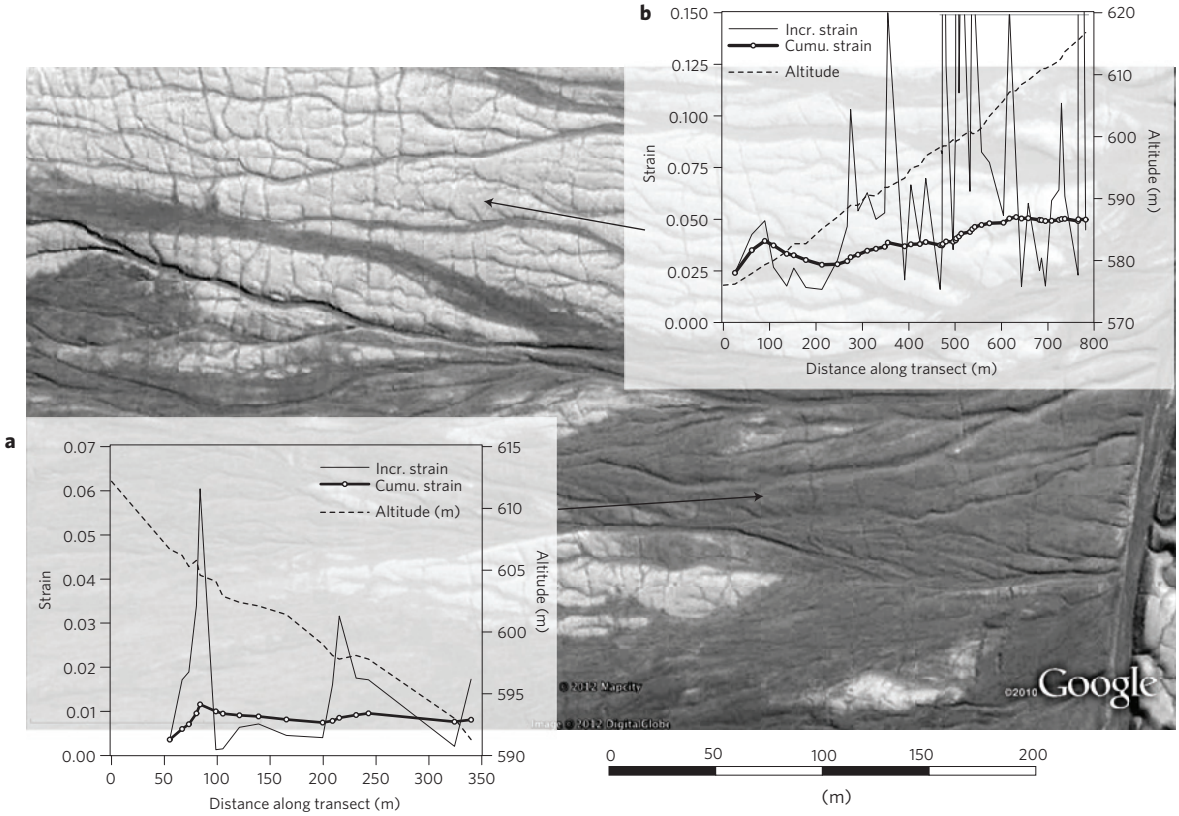

Figure 2 | Surface cracks at Punta de Lobos. Detail of Google Earth image showing differing crack densities in the oldest and youngest dated surface, and two representative scan line plots showing incremental and cumulative strain as well as elevation variation along the scan line. **a**, One of the scan lines from the S5 surface (<0.2 Myr). **b**, A scan line from the S1 surface (~0.9 Myr). Similar plots for the remainder of the scan line data for Punta de Lobos can be found in the Supplementary Information.

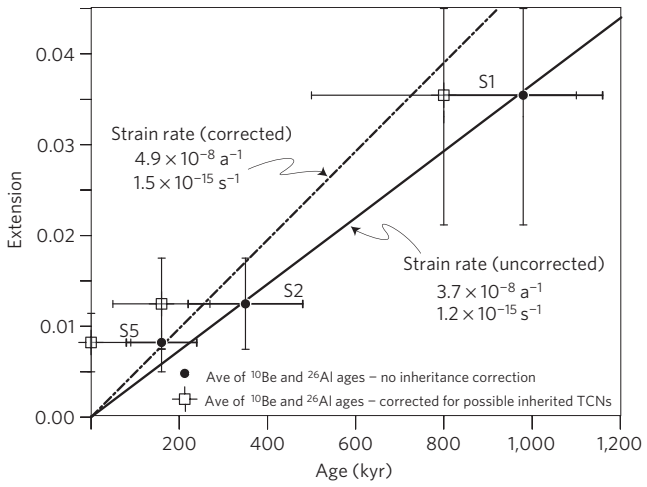

Figure 3 | Strain rate due to surface cracks at Punta de Lobos. Strain from scan line measurements of crack apertures on fan surfaces as a function of TCN surface exposure ages. 1σ error bars are described in Supplementary Tables S1 and S2. Slopes were calculated using a least-squares best fit that was constrained to go through the origin; the corrected strain rate uses the ages and errors that have been corrected for possible inherited TCN values whereas the uncorrected strain rate uses the raw TCN ages and errors without any inheritance correction as described in the Supplementary Information. Note the linear nature of the relationships, suggesting a consistent strain rate for the last ~800–1,000 kyr.

magnitudes because the length scales are different. The average length change across 50 km perpendicular to the coast for Maule was 2.6 m and for Antofagasta was about 40 cm. The Punta de Lobos fan complex is 1,250 m wide so the 150 year event would produce 8.9 mm and the 300 year event 1.78 cm of length change. If cracking occurred only at Punta de Lobos and nowhere else in the region, then the absolute minimum permanent component would be 0.37–0.74% of GPS measured deformation for a Maule-sized event, and 2.3–4.6% of an Antofagasta-sized event (in all cases the two figures are for the 150 and 300 year events).

However, it is unreasonable to assume that cracking occurs only on the Punta de Lobos fan as extensive crack development is present throughout the greater region[22], although we lack similar age control elsewhere. If we assume that 10% of the region has a crack strain equivalent to Punta de Lobos, then the proportion of the total GPS strain that was due to permanent cracking would be 1.5–3% for a Maule-sized event and 9–18% for an Antofagasta-sized event (although Antofagasta was almost certainly not a 300 year event and thus 18% is probably unreasonable).

It is also likely that some of the cracking is due to upper-plate faulting. Nearby east-striking reverse faults such as at Chuculay probably form during the interseismic part of the subduction earthquake cycle and have extensive cracks, which were not included in this study[20,26]. The Punta de Lobos fan complex is located next to a steep, north-striking eponymous normal fault. The post-seismic earthquake activity at Pichilemu (Fig. 4) following the 2010 Maule earthquake[27–29] shows that normal faulting can form co/post-seismically and affects the deeper

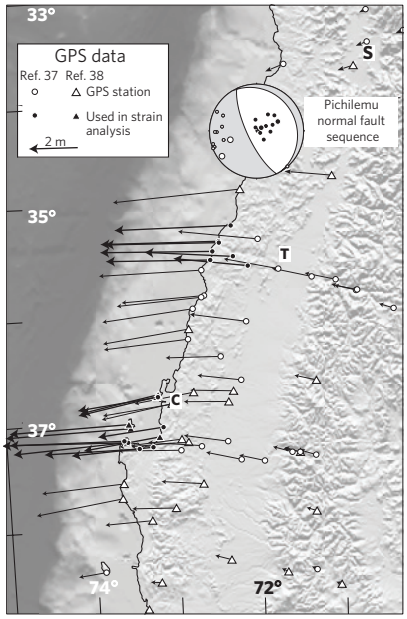

Figure 4 | Co/post-seismic GPS data for the 2010 Maule earthquake. Individual vectors from ref. 37 (circle station symbols) and ref. 38 (triangle symbols). Stations used in the strain analysis (Fig. 5 and Supplementary Fig. S9) are filled black with heavy arrow; others are hollow. Also shown is a composite focal mechanism for the Pichilemu normal fault aftershock sequence constructed by summing the moment tensors[29]. Dots show individual P (solid) and T (hollow) axes; larger dots are the M_w 6.9 and 7.0 main shocks. Lower hemisphere projection is centred on the Pichilemu structure.

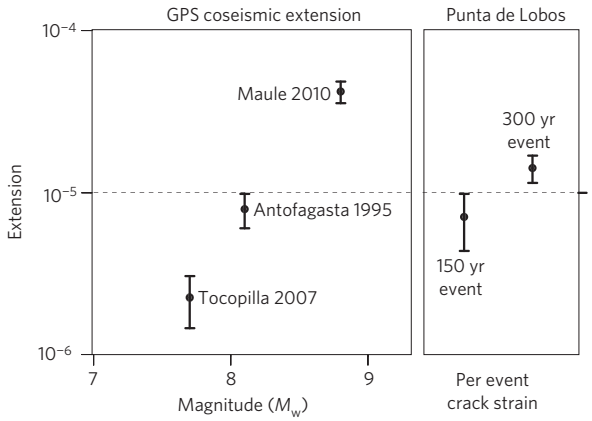

Figure 5 | Strain magnitude from cracks and co/post-seismic GPS data. Comparison of 2D co/post-seismic extensional strains from GPS and field measurements of co/post-seismic cracks. The GPS strains were measured from the 1D coseismic displacement gradients in the 50 km immediately east of the coastline. GPS strain calculated from data in refs 15,36–38. The crack strain and associated errors are calculated for a 150- and 300-year average recurrence interval as discussed in the text. The calculation of errors and GPS strain is described in the Supplementary Information.

levels of the forearc crust, not just the surface. If the Punta de Lobos normal fault and the many other normal faults in the Coastal Cordillera[20,23,30–33] also move co/post-seismically to plate-boundary earthquakes, then their heaves would have to be added to the crack strain in accounting for total permanent co/post-seismic deformation.

Permanent forearc extension during each subduction earthquake requires either that the upper plate stretches with time or there is permanent shortening during some part of the seismic cycle. We suggest that two processes are at play: first, some of the permanent extension is counteracted by thrust fault reactivation of forearc normal faults[20,34], most likely during the interseismic part of the cycle. Although we cannot estimate the total shortening due to thrust reactivation, the morphology and fault dips alone suggest that it is significantly smaller than the normal fault zones in which they occur. Second, co/post-seismic extension contributes to the stretching and break-up of the northern Chile forearc, which will facilitate subsequent subduction erosion of the margin[31,35]. If the plate boundary is fully locked during the interseismic period, then subduction erosion could happen only during the co/post-seismic phase.

We conclude that between ~1.5 and 10% of the 1D, horizontal GPS-recorded coseismic strain is probably permanent. Whereas coseismic rebound may well be predominantly elastic at deeper levels in the crust, both the cracks and the GPS stations on which the geodetic coseismic strain estimates are based measure surface strains. This rate of permanent forearc deformation has persisted for nearly 1 Myr over 400–500 km of margin length, produced by 2,000 to 9,000 individual earthquake cycles. This study complements those documenting permanent vertical uplift of the forearc[4]. Together, they suggest that co/post-seismic rebound includes a significant plastic component and thus highlight the need to re-evaluate the use of purely elastic or viscoelastic modelling of GPS data for determining slip magnitudes, interseismic coupling models and other indirectly measured parameters of major subduction zone earthquakes.

Received 6 June 2012; accepted 5 March 2013; published online 28 April 2013

References

1. Reid, H. F. in *The California Earthquake of April 18, 1906* Vol. 2 (ed. Lawson, A. C.) (Carnegie Institution, 1910).
2. Wang, K., Hu, Y. & He, J. Deformation cycles of subduction earthquakes in a viscoelastic Earth. *Nature* **484,** 327–332 (2012).
3. Thatcher, W. & Rundle, J. B. A viscoelastic coupling model for the cyclic deformation due to periodically repeated earthquakes at subduction zones. *J. Geophys. Res.* **89,** 7631–7640 (1984).
4. Bookhagen, B., Echtler, P., Melnick, D., Strecker, R. & Spencer, J. Q. G. Using uplifted Holocene beach berms for paleoseismic analysis on the Santa María Island, south-central Chile. *Geophys. Res. Lett.* **33,** L15302 (2006).
5. Dunai, T. J., González López, G. A. & Juez-Larré, J. Oligocene–Miocene age of aridity in the Atacama Desert revealed by exposure dating of erosion-sensitive landforms. *Geology* **33,** 321–324 (2005).
6. Hartley, A. J. & Chong, G. Late Pliocene age for the Atacama Desert: Implications for the desertification of western South America. *Geology* **30,** 43–46 (2002).
7. Placzek, C. J., Matmon, A., Granger, D. E., Quade, J. & Niedermann, S. Evidence for active landscape evolution in the hyperarid Atacama from multiple terrestrial cosmogenic nuclides. *Earth Planet. Sci. Lett.* **295,** 12–20 (2010).
8. Rech, J. A., Currie, B. S., Michalski, G. & Cowan, A. M. Neogene climate change and uplift in the Atacama Desert, Chile. *Geology* **34,** 761–764 (2006).
9. Pritchard, M. E., Simons, M., Rosen, P. A., Hensley, S. & Webb, F. H. Co-seismic slip from the 1995 July 30 $M_w = 8.1$ Antofagasta, Chile, earthquake as constrained by InSAR and GPS observations. *Geophys. J. Int.* **150,** 362–376 (2002).
10. Pritchard, M. E. *et al.* Geodetic, teleseismic, and strong motion constraints on slip from recent southern Peru subduction zone earthquakes. *J. Geophys. Res.* **112,** B03307 (2007).
11. Delouis, B. *et al.* The $M_w = 8.0$ Antofagasta (Northern Chile) earthquake of 30 July 1995: A precursor to the end of the large 1877 gap. *Bull. Seismol. Soc. Am.* **87,** 427–445 (1997).
12. Beck, S. L. & Ruff, L. J. Great earthquakes and subduction along the Peru Trench. *Phys. Earth Planet. Int.* **57,** 199–224 (1989).
13. Comte, D. & Pardo, M. Reappraisal of great historical earthquakes in the northern Chile and southern Peru seismic gaps. *Nature Hazards* **4,** 23–44 (1991).
14. Lomnitz, C. Major earthquakes of Chile: A historical survey, 1535–1960. *Seismol. Res. Lett.* **75,** 368–378 (2004).

15. Béjar-Pizarro, M. *et al.* Asperities and barriers on the seismogenic zone in North Chile: state-of-the-art after the 2007 M_w 7.7 Tocopilla earthquake inferred by GPS and InSAR data. *Geophys. J. Int.* **183,** 390–406 (2010).
16. Delouis, B., Pardo, M., Legrand, D. & Monfret, T. The M_w 7.7 Tocopilla earthquake of 14 November 2007 at the southern edge of the northern Chile seismic gap: Rupture in the deep part of the coupled plate interface. *Bull. Seismol. Soc. Am.* **99,** 87–94 (2009).
17. Angermann, D., Klotz, J. & Reigber, C. Space-geodetic estimation of the Nazca–South America Euler Vector. *Earth Planet. Sci. Lett.* **171,** 329–334 (1999).
18. Kendrick, E. *et al.* The Nazca–South America Euler vector and its rate of change. *J. S. Am. Earth Sci.* **16,** 125–131 (2003).
19. Loveless, J. P., Allmendinger, R. W., Pritchard, M. E., Garroway, J. L. & González, G. G. Surface cracks record long-term seismic segmentation of the Andean margin. *Geology* **37,** 23–26 (2009).
20. Allmendinger, R. W. & González, G. G. Neogene to Quaternary Tectonics of the Coastal Cordillera, northern Chile. *Tectonophysics* **495,** 93–110 (2010).
21. Keefer, D. K. & Moseley, M. E. Southern Peru desert shattered by the great 2001 earthquake: Implications for paleoseismic and paleo-El Niño southern oscillation records. *Proc. Natl Acad. Sci. USA* **101,** 10878–10883 (2004).
22. Loveless, J. P. *et al.* Pervasive cracking of the northern Chilean Coastal Cordillera: New evidence of forearc extension. *Geology* **33,** 973–976 (2005).
23. González, G., Cembrano, J., Carrizo, D., Macci, A. & Schneider, H. The link between forearc tectonics and Pliocene-Quaternary deformation of the Coastal Cordillera, northern Chile. *J. S. Am. Earth Sci.* **16,** 321–342 (2003).
24. Marquardt, C., Naranjo, J. A. & Lavenu, A. Efectos geológicos del sismo del 13 de junio 2005, región de Tarapacá. *XI Congr. Geol. Chileno* **2,** 435–438 (2006).
25. Quezada, J. *et al.* Comment to Nature and tectonic significance of co-seismic structures associated with the M_w 8,8 Maule earthquake, central-southern Chile forearc from Arriagada *et al.* (2011). *J. Struct. Geol.* **37,** 253–255 (2012).
26. González, G. *et al.* Crack formation on top of propagating reverse faults of the Chuculay Fault System northern Chile: Insights from field data and numerical modelling. *J. Struct. Geol.* **30,** 791–808 (2008).
27. Farías, M., Comte, D., Roecker, S., Carrizo, D. & Pardo, M. Crustal extensional faulting triggered by the 2010 Chilean Earthquake: The Pichilemu seismic sequence. *Tectonics* **30,** TC6010 (2011).
28. Ryder, I. *et al.* Large extensional aftershocks in the continental forearc triggered by the 2010 Maule earthquake, Chile. *Geophys. J. Int.* **188,** 879–890 (2012).
29. Aron, F., Allmendinger, R., Cembrano, J., González, G. & Yáñez, G. Permanent forearc extension and seismic segmentation: Insights from the 2010 Maule earthquake, Chile. *J. Geophys. Res.* **118,** http://dx.doi.org/10.1029/2012JB009339 (2013).
30. Arabasz, W. J. *Geological and geophysical studies of the Atacama fault zone in northern Chile*, PhD thesis (California Institute of Technology, 1971).
31. Armijo, R. & Thiele, R. Active faulting in northern Chile; ramp stacking and lateral decoupling along a subduction plate boundary? *Earth Planet. Sci. Lett.* **98,** 40–61 (1990).
32. Delouis, B., Philip, H., Dorbath, L. & Cisternas, A. Recent crustal deformation in the Antofagasta region (northern Chile) and the subduction process. *Geophys. J. Int.* **132,** 302–338 (1998).
33. Niemeyer, H., González, G. & Martínez-De Los Ríos, E. Evolución tectónica cenozoica del margen continental activo de Antofagasta, norte de Chile. *Rev. Geol. Chile* **23,** 165–186 (1996).
34. Loveless, J. P., Allmendinger, R. W., Pritchard, M. E. & González, G. Normal and reverse faulting driven by the subduction zone earthquake cycle in the northern Chilean fore arc. *Tectonics* **29,** TC2001 (2010).
35. von Huene, R. & Ranero, C. R. Subduction erosion and basal friction along the sediment-starved convergent margin off Antofagasta, Chile. *J. Geophys. Res.* **108,** 2079 (2003).
36. Klotz, J. *et al.* GPS-derived deformation of the Central Andes including the 1995 Antofagasta M_w = 8.0 Earthquake. *Pure Appl. Geophys.* **154,** 709–730 (1999).
37. Vigny, C. *et al.* The 2010 M_w 8.8 Maule megathrust earthquake of Central Chile, monitored by GPS. *Science* **332,** 1417–1421 (2011).
38. Moreno, M. *et al.* Toward understanding tectonic control on the M_w 8.8 2010 Maule Chile earthquake. *Earth Planet. Sci. Lett.* **321-322,** 152–165 (2012).

Acknowledgements

This material is based on work supported by the National Science Foundation under Grant No. EAR-0738507. We are grateful to G. González, M. Pritchard, J. Loveless and F. Aron for long-term collaboration and discussion of the ideas presented here. Many thanks to M. Caffee and staff at PRIME Laboratory, Purdue University for making the AMS measurements for ^{10}Be and ^{26}Al.

Author contributions

The field research and geochemical analyses described here were performed by A.B., with further field observations and consultation by R.W.A., L.A.O. and J.A.R. Samples were processed in L.A.O.'s laboratory and data and error analyses were reviewed and calculated by L.A.O., R.W.A. and A.B. Analyses of geodetic and crack strain were performed by R.W.A. The manuscript was written by R.W.A. based in part on text provided by A.B., and was edited by L.A.O. and J.A.R.

Additional information

Supplementary information is available in the online version of the paper. Reprints and permissions information is available online at www.nature.com/reprints. Correspondence and requests for materials should be addressed to R.W.A.

Competing financial interests

The authors declare no competing financial interests.